

by

$$\begin{aligned} c\pi\nu^+ &= \delta e + \delta^2 k, & cK\nu^+ &= \delta d + \delta^2 l, \\ K\nu^0 &= \frac{1}{3}\delta^2(e^*d + f^*g), & c\eta\nu/\sqrt{3} &= \frac{1}{2} - \frac{1}{6}\delta^2(|d|^2 + |g|^2), \\ c\pi\nu^0 &= \frac{3}{2} - \frac{1}{3}\delta^2(|e|^2 + |f|^2 + \frac{1}{2}|d|^2 + \frac{1}{2}|g|^2), \\ c\pi^+ &= \delta f + \delta^2 m, & cK^+ &= \delta g + \delta^2 n, \\ cK^0 &= \frac{1}{3}\delta^2(e^*g + df^*), & c\eta/\sqrt{3} &= -\frac{1}{6}\delta^2(dg^* + d^*g), \\ c\pi^0 &= -\frac{1}{3}\delta^2(ef^* + e^*f + \frac{1}{2}dg^* + \frac{1}{2}d^*g), \end{aligned}$$

where $d, e, f, g, k, l, m,$ and n are arbitrary. A solution that gives the proper Cabibbo angle is obtained by setting $e=4d$ and $f=4g$, and $k=l=m=n=0$ (for

simplicity):

$$\begin{aligned} c\pi\nu^+ &= 4\delta d, & cK\nu^+ &= \delta d, \\ cK\nu^0 &= \frac{4}{3}\delta^2(|d|^2 + |g|^2), & c\eta\nu/\sqrt{3} &= \frac{1}{2} - \frac{1}{6}\delta^2(|d|^2 + |g|^2), \\ c\pi\nu^0 &= \frac{3}{2} - \frac{1}{3}\delta^2(|d|^2 + |g|^2), & c\pi^+ &= 4\delta g, \\ cK^+ &= \delta g, & cK^0 &= 8/3\delta^2 \operatorname{Re}(d^*g), \\ c\eta/\sqrt{3} &= -\frac{1}{3}\delta^2 \operatorname{Re}(d^*g), & c\pi^0 &= -11\delta^2 \operatorname{Re}(d^*g). \end{aligned}$$

One notes that the amplitudes $c\eta\nu$ and $c\pi\nu^0$ are arbitrarily larger than the amplitudes $c\pi\nu^+, cK\nu^+, c\pi^+$, and cK^+ which in turn are arbitrarily larger than the $c\eta, c\pi^0, cK\nu^0,$ and cK^0 amplitudes. The consequence of electromagnetic interaction $\pi\nu^0 = \sqrt{3}\eta\nu$ is violated in the second order in δ .

Nucleon Isobar Excitation in $\pi^\pm p$ Scattering*

ARCHIBALD W. HENDRY† AND J. S. TREFIL

Department of Physics, University of Illinois, Urbana, Illinois 61801

(Received 17 March 1969)

The major differences in the differential cross sections for $\pi p \rightarrow \pi p, \pi p \rightarrow \pi N^*(1.4)$ and $\pi p \rightarrow \pi N^*(1.69)$ are explained on the basis of composite structure for the nucleon and its isobars.

TWO significant features are observed¹ in experimental investigations of the reactions $\pi p \rightarrow \pi N^*(1.4)$ and $\pi p \rightarrow \pi N^*(1.69)$.

(a) At small t , the inelastic differential cross sections are more than an order of magnitude smaller than the elastic cross section.

(b) The slopes of the differential cross sections are vastly different. If we write $d\sigma/dt = Ae^{Bt}$, then B is about 8 (GeV/c)⁻² for elastic scattering. In direct contrast, B is 12–16 (GeV/c)⁻² for $N^*(1.4)$ production (corresponding to a much steeper forward peak), whereas for $N^*(1.69)$ the data are consistent with a flat distribution.

In this paper, we show how these striking features can be explained in a very natural way on the basis of quark-model wave functions² for the different N^* states. We shall see that the difference between the $N^*(1.4)$ and the $N^*(1.69)$ production arises because the former is essentially a radial excitation of the three-quark system, while the latter is an orbital excitation.

To describe the scattering from a composite system, we shall use the Glauber theory,³ which has frequently been used with success in the description of particle production from nuclei.⁴ The proton is to be regarded as a three-quark system which the scattering can either leave in its ground state (elastic scattering) or excite⁵ (isobar production). In order to simplify the calculation and to emphasize the simplicity of the mechanism which we are proposing to explain the data on isobar production, we treat the pion as an elementary particle.⁶ Our concern here is with the general features of the model and not with detailed fitting of the data.

The basic assumption of the Glauber theory is that, in scattering from a complex system, the phase shift for

³ R. J. Glauber, in *Lectures in Theoretical Physics*, edited by W. E. Britten and L. G. Dunham (Wiley-Interscience Inc., New York, 1959), Vol. 1; and *High Energy Physics and Nuclear Structure* (North-Holland Publishing Co., Amsterdam, 1967).

⁴ J. Formánek and J. S. Trefil, *Nucl. Phys.* **B3**, 155 (1967); **B4**, 165 (1965). B. Margolis, *Phys. Letters* **26B**, 524 (1968); *Nucl. Phys.* **B4**, 433 (1968). J. S. Trefil, *Phys. Rev.* **180**, 1366 (1969); **180**, 1379 (1969).

⁵ Our use of definite target wave functions distinguishes our method from that of several others who have combined the eikonal approximation with Regge exchange; see, e.g., S. Frautschi and B. Margolis, *Nuovo Cimento* **57A**, 427 (1968); C. B. Chiu and J. Finkelstein, *Nuovo Cimento* **57**, 649 (1968). Some of our results, however, have features in common with the coherent droplet model; see, e.g., R. C. Arnold, *Phys. Rev.* **157**, 1292 (1967).

⁶ Work is in progress in which the pion is also treated as a composite system. Our initial investigations indicate little change from the results quoted here. Obviously, in proton-proton collisions, both projectile and target must be taken as composites.

* Supported in part by the National Science Foundation under Grant No. NSF GP-9273.

† Present address: Physics Dept., Indiana University, Bloomington, Ind. 47401.

¹ K. J. Foley, R. S. Jones, S. J. Lindenbaum, W. A. Love, S. Ozaki, E. D. Platner, C. A. Quarles, and E. H. Willen, *Phys. Rev. Letters* **19**, 397 (1967).

² D. Faiman and A. W. Hendry, *Phys. Rev.* **173**, 1720 (1968); **180**, 1609 (1969).

the scattering from the system as a whole is given by the sum of the phase shifts for the scattering from the individual constituents. With this assumption, it is possible to derive an expression for the scattering amplitude from a complex system in terms of the scattering amplitudes for scattering from the constituents. In the present case, the amplitude which takes the proton target from the state ψ_i to a final state ψ_f is given by

$$\mathcal{F} = \frac{i\hat{p}}{2\pi} \langle \psi_f | \int d\mathbf{b} e^{i\Delta \cdot \mathbf{b}} \times (3F_j - 3c_2 F_j F_k + c_3 F_j F_k F_l) | \psi_i \rangle, \quad (1)$$

where

$$F_j = \frac{1}{2\pi i \hat{p}_j} \int d\delta_j e^{i\delta_j \cdot (\mathbf{b} - \mathbf{s}_j + \mathbf{s})} e^{i\Delta_m(z_j - z)} f_j(\delta_j).$$

In these expressions, Δ is the transverse momentum transfer and $\Delta_m \approx (m_f^2 - m_i^2)/2p_{lab}$ is the longitudinal momentum transfer associated with the change in mass of the baryon. In the usual Gartenhaus-Schwartz scheme,⁷ the position of the j th quark is $\mathbf{r}_j = \mathbf{s}_j + \mathbf{z}_j$, and $\mathbf{s} = \Sigma \mathbf{s}_j/A$, $z = \Sigma z_j/A$. The constants c_2 , c_3 are unity for elastic scattering, and $c_2 = 2$, $c_3 = 3$ for inelastic processes, taking into account the fact that in n th-order scattering, the target may be excited by exciting any of the n struck quarks.

In our calculations, the pion-quark scattering amplitude f_j was expressed as

$$f_j(\delta_j) = [(i + \beta)/4\pi] \sigma_{\pi q} \exp(-\frac{1}{2} a \delta_j^2), \quad j = 1, 2, 3$$

where δ_j is the momentum transfer at the constituent j . The parameters σ , β , and a were taken as constants (independent of energy) since all the processes we consider can proceed via Pomeron exchange. Spin effects are neglected.

Next we have to specify the wave functions of the target for both its ground state and the states corresponding to $N^*(1.4)$ and $N^*(1.69)$. As a working hypothesis,⁸ we shall take the wave functions as given by the symmetric harmonic-oscillator model for baryons.^{2,9,10} This model has enjoyed considerable success, particularly in accounting for the observed spectrum of nucleon resonances. In this scheme, the ground-state nucleon has the spatial configuration $(1s)^2$, $56 L=0^+$.¹¹ The $N^*(1.4)$, which is the well-known P_{11} Roper resonance, is expected^{2,10} to belong primarily to the configuration $(1s)(2s)$, $56 L=0^+$, that is, a radial excitation (in the relative coordinates) of the nucleon. For the $N^*(1.69)$ we take the wave function $(1s)(1d)$, $56 L=2^+$, which is appropriate to the $F_{15}(1.69)$ resonance. There are, in fact, several resonances in this mass region, and the experiments do not separate them. However, since the

⁷ S. Gartenhaus and C. L. Schwartz, Phys. Rev. **108**, 482 (1957).

⁸ The general features of our results are not particularly dependent on the use of harmonic-oscillator wave functions.

⁹ O. W. Greenberg, Phys. Rev. Letters **13**, 598 (1964).

¹⁰ R. H. Dalitz, in Proceedings of the Conference on High-Energy Physics, University of California (Irvine), 1967 (unpublished).

¹¹ The harmonic-oscillator levels referred to here are with respect to oscillations in the two relative coordinates.

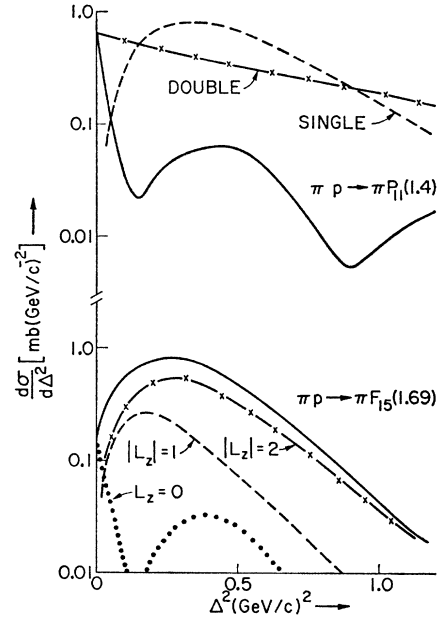


FIG. 1. Predictions of our model for the reactions $\pi N \rightarrow \pi P_{11}(1.4)$ (upper curves) and $\pi N \rightarrow \pi F_{15}(1.69)$ (lower curves). In the former, we show the effects of the interference between single and double scattering, while in the latter, we show the amplitudes corresponding to different values of L_z . In both cases, the heavy line represents the sum of all multiple-scattering terms.

F_{15} is the first Regge recurrence of the nucleon and has the right quantum numbers for Pomeron exchange, it seems likely that at high energies this resonance will yield a major contribution to the experimental data.

The explicit wave functions for these states are listed

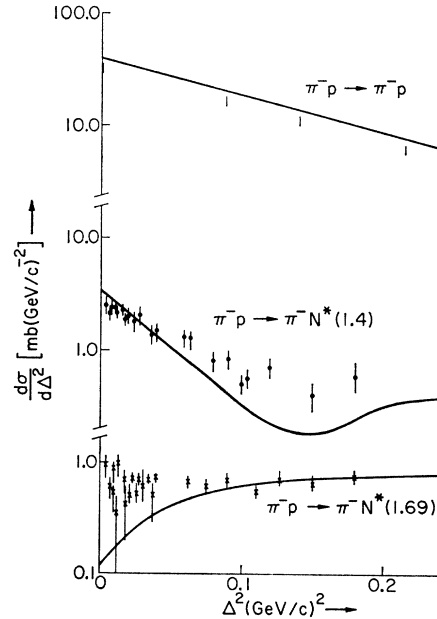


FIG. 2. Comparison of our model with the data of Ref. 1. The data represent lab momenta from 14 to 26 GeV/c. (There are no significant energy-dependent effects observable.)

in Ref. 2. The various differential cross sections may now be calculated directly by inserting these wave functions into Eq. (1) and performing the necessary integrals, all of which can be done analytically. Rather than quote the resulting amplitudes, we shall describe our results graphically by means of Figs. 1 and 2.

In Fig. 1, we show the differential cross sections for isobar production as calculated according to Eq. (1). The single- and double-scattering contributions are drawn separately for the P_{11} case to illustrate a very important feature in isobar production, namely, that the single-scattering term *vanishes* at $\Delta^2=0$. This is a general property which is shared by all composite models of the baryons since, in this limit, the matrix element $\langle \psi_f | e^{i\Delta \cdot r} | \psi_i \rangle$ must go to zero because of the orthogonality of the physical states. Since the single-scattering term dominates the elastic scattering at small Δ , the absence of this term in isobar production provides a simple explanation of the difference in magnitudes between the two [experimental feature (a) above]

To investigate the shapes of the differential cross sections, we must look in more detail at higher-order multiple-scattering terms. Unlike single scattering, these need not vanish at $\Delta^2=0$ in isobar production.¹² In elastic scattering, it is well known^{3,4} that the interference between the single and double terms produces a diffraction minimum at the point where the two terms are equal, since they have a relative minus sign between them. Such minima (or, more typically, shoulders) occur at momentum transfers much greater than 0.2 (GeV/c)², usually,¹³ in fact, at about 1 (GeV/c)². For $N^*(1.4)$ production, we can immediately see the significance of the vanishing of the single scattering at $\Delta^2=0$. Now there are two places where the single and double scatterings are of equal magnitude—one at small t where the single-scattering term is rising as well as the usual one at larger t where the single-scattering term is falling. Thus the model predicts two diffraction minima in $\pi p \rightarrow \pi N^*(1.4)$ for $|t| \lesssim 1$ (GeV/c)², as opposed to only one minimum in elastic scattering. For values of t below the first minimum around 0.2 (GeV/c)², the slope of the differential cross section for $N^*(1.4)$ production is very steep.

For $F_{15}(1.69)$ production, we must take into account all of the components $|L_z|=0, 1,$ and 2 in the F_{15} wave function. As shown in Fig. 1, the contribution from $L_z=0$ is similar to the $N^*(1.4)$ production above. The $|L_z|=1$ and 2 contributions, on the other hand, rise from zero as $|t|$ increases (all of the terms in their multiple-scattering series are proportional to Δ). Altogether, therefore, the final shape has a dip in the for-

ward direction; the curve flattens off, then falls exponentially.

With this qualitative understanding of the various effects, we turn to a comparison with the experimental data.^{1,14} If the parameters $\sigma, \beta,$ and a are fixed by fitting to the elastic πp data,¹⁵ the magnitudes and slopes of the N^* differential cross sections then follow as *consequences*. Our results are shown in Fig. 2. We see that the experimentally observed steep slope of the $N^*(1.4)$ cross section is matched reasonably well by our model, and likewise the flat differential cross section at large Δ^2 for $N^*(1.69)$ production. The dip which we anticipate at very small t for the latter reaction is not inconsistent with the data.

There are, however, difficulties over absolute normalization when making a comparison with the $N^*(1.4)$ data: The model predicts a value of $d\sigma/dt$ at $t=0$ which is a factor of about 4 below the experimentally reported value. Because of the rather large systematic uncertainties (primarily due to background separation) of the experimental data itself, it was not thought that a theoretical attempt to resolve this problem was necessary at the present time [although such an attempt could be made, for example, by introducing configuration mixing between the $N^*(1.4)$ and the nucleon]. We have therefore renormalized our theoretical curve for $N^*(1.4)$ in Fig. 2. The calculated curve for F_{15} production lies close to the numbers quoted in Ref. 1. for $N^*(1.69)$ production without any change in normalization.

Thus we find that this model, in which the nucleon and its $N^*(1.4), N^*(1.69)$ resonances are treated as composite systems, provides simple explanations for all the outstanding features of the isobar production data. Depending on the scale factor to be applied to the experimental data for the inelastic processes, it would also appear to be quantitatively reasonable. In addition, the following hard predictions come from the model.

(a) At higher energies where contamination from nondiffractive isobars disappears, a shallow dip will appear in the reaction $\pi N \rightarrow \pi F_{15}(1.69)$ at small t .

(b) When the reaction $\pi N \rightarrow \pi N^*(1.4)$ is measured at larger momentum transfers, the differential cross section will display a diffraction minimum at $|t| \approx 0.2$ (GeV/c)², then a shoulder followed by a second diffraction minimum at about 1 (GeV/c)².

(c) If higher mass nucleon excitations are found, we expect, by analogy with the results presented here, that those corresponding to pure radial excitations in the quark scheme will exhibit sharp forward peaks [like the $N^*(1.4)$], while those corresponding to pure orbital excitations will display relatively flat differential cross sections.

¹² That the double scattering need not vanish at $\Delta^2=0$ can easily be seen by noting that it is possible in this case to transfer momentum $+\mathbf{q}$ to the first particle and $-\mathbf{q}$ to the second. The matrix element $\langle \psi_f | e^{i\mathbf{q} \cdot \mathbf{r}_1} e^{-i\mathbf{q} \cdot \mathbf{r}_2} | \psi_i \rangle$ is not, in general, zero.

¹³ For an investigation of elastic scattering and the observed structure for $\Delta^2 \gtrsim 1$ (GeV/c)², see D. R. Harrington and A. Pagnamenta, Phys. Rev. Letters **18**, 1147 (1967); Phys. Rev. **173**, 1599 (1968); A. Deloff, Nucl. Phys. **B2**, 597 (1967).

¹⁴ For reference, we use the π^-p data (Ref. 1); the π^+p data are similar but less abundant.

¹⁵ For the fit shown, $\sigma=10.5$ mb, $\beta=-0.16$, and $a=2.25$ (GeV/c)⁻². The spring constant of the harmonic oscillator was chosen to correspond to a rms radius of 0.8 F for the nucleon.